Int. J. Electrochem. Sci., 15 **(2020)** 959 – 965, doi: 10. 20964/2020.01.53

International Journal of ELECTROCHEMICAL SCIENCE
www.electrochemsci.org

Short Communication

A Novel Cobalt-free $La_{0.6}Sr_{0.4}Fe_{0.9}Nb_{0.1}O_3$ Cathode for Medium Temperature Solid Oxide Fuel Cells

Huihuang Jiang[1], *Feng Zhang*[2,*]

[1] School of Art, Soochow University, Suzhou 215123, PR China
[2] Analysis and Testing Center, Soochow University, Suzhou 215123, PR China
[*]E-mail: ylfengzhang@suda.edu.cn

Received: 30 August 2019 / *Accepted:* 8 November 2019 / *Published:* 30 November 2019

A novel cobalt-free $La_{0.6}Sr_{0.4}Fe_{0.9}Nb_{0.1}O_3$ (LSFNb) cathode material was synthesized by a solid-state reaction. And $BaCe_{0.7}Zr_{0.2}Sm_{0.1}O_{3-\alpha}$ (BCZSm) electrolyte was prepared by a sol-gel method. Transmission Electron Microscopy (TEM) and Thermal Gravimetry Analysis-Differential Scanning Calorimetry (TGA-DSC) were used to determine the size and the first sintering temperature of BCZSm, respectively. The structures of cathode, electrolyte and anode were analyzed via X–ray Diffraction (XRD). A thin film fuel cell of LSFNb / BCZSm / NiO-BCZSm was assembled and reached the highest power densities of 109 $mW \cdot cm^{-2}$ and 182.6 $mW \cdot cm^{-2}$ at 700 °C and 800 °C, respectively.

Keywords: Electrolyte; Fuel cell; X–ray diffraction; Solid state reaction

1. INTRODUCTION

Fuel cells play an important role in the development of clean energy due to their high efficiency and low pollution [1–6]. A solid oxide fuel cell (SOFC) is a fully solid-state device consisting of an anode, cathode and electrolyte [7–10]. The cathode catalyzes oxygen into oxygen ions and transfers them to the electrolyte interface. The cathode materials require a porous structure, good stability and mixed conductivity in working temperature range [11–13]. At present, research on SOFC cathode materials mainly focuses on perovskite oxides, mainly ABO_3 and A_2BO_4 type oxides. Co-containing perovskite-oxides such as $La_{1-x}Sr_xCoO_3$ (LSC) are the main candidate materials for SOFC cathode materials due to their excellent electronic-ionic mixed conductivities. The development of Fe doped at Co site has become a common research direction. However, $La_{1-x}Sr_xCo_{1-y}Fe_yO_3$ (LSCF) has a high coefficient of thermal expansion. Therefore, the search for new high performance Co-free cathode materials has become a hot spot in the development of SOFC [14–15]. We previously reported a Co-

free cathode material, $La_{0.6}Sr_{0.4}Fe_{1-x}Ni_xO_{3-\alpha}$, which had a good fuel cell performance [16]. In recent years, researchers have found that the use of high valence metal cations can improve the performance of cathode materials, such as $(La_{0.6}Sr_{0.4})_{1-x}Co_{0.2}Fe_{0.6}Nb_{0.2}O_{3-\alpha}$, $La_{0.9}Ca_{0.1}Fe_{0.9}Nb_{0.1}O_{3-\alpha}$, etc. [17–20].

Electrolyte is a core component of a fuel cell [21–23]. In terms of carrier transport, H^+ transmission resistance is much less than O^{2-}. At present, research into proton conductor materials mainly focuses on $BaZrO_3$ and $BaCeO_3$-based materials. It has been reported that $BaCeO_3$ and $BaZrO_3$ can form infinite solid solution $BaZr_xCe_{1-x}O_3$. And it has been confirmed that doping of low-valent elements can improve the proton conductivity of the material. The effective ionic radius of Sm^{3+} is close to that Ce^{4+}. In order to mix the raw materials at the molecular level, electrolytes are usually synthesized by liquid phase method [24–26].

In this paper, novel cathode material, $La_{0.6}Sr_{0.4}Fe_{0.9}Nb_{0.1}O_3$ (LSFNb) was synthesized. The electrolyte of $BaCe_{0.7}Zr_{0.2}Sm_{0.1}O_{3-\alpha}$ (BCZSm) was prepared by sol-gel method. Electrolyte films were prepared on anode substrates and the electrochemical performance of ceramic membrane fuel cells was studied.

2. EXPERIMENTAL

$La_{0.6}Sr_{0.4}Fe_{0.9}Nb_{0.1}O_3$ (LSFNb) was prepared by high temperature solid-state method. According to the stoichiometric ratio, La_2O_3, $SrCO_3$, Fe_2O_3 and Nb_2O_5 were mixed uniformly and annealed at 1000 °C and 1150 °C for 5 h to obtain LSFNb. The cathode slurry was prepared by mixing the prepared LSFNb with an appropriate amount of binder (ethyl cellulose and terpineol).

$BaCe_{0.7}Zr_{0.2}Sm_{0.1}O_{3-\alpha}$ (BCZSm) was synthesized via a facile sol-gel method using citric acid as a chelating agent. The amounts of raw materials ($Ba(NO_3)_2$, citric acid, Sm_2O_3, $(NH_4)_2Ce(NO_3)_6$ and $Zr(NO_3)_4{\cdot}5H_2O$) were calculated according to stoichiometric ratio. Sm_2O_3 was dissolved in hot diluted nitric acid solution to form $Sm(NO_3)_3$ solution. The molar ratio of citric acid to total metal ions was controlled at 2:1. With the evaporation of water, the concentration of the solution increased gradually to a viscous gelatin. The gel was heated to form a fluffy powder and calcinated at 1100 °C and 1400 °C for 5 h, respectively. The electrolyte slurry was prepared by grinding BCZSm powder and organic binder at a mass ratio of 30:70 for 2 h.

NiO and BCZSm powders were milled at a mass ratio of 60:40 for 2 h, then 15% of activated carbon was added as a pore-forming agent. The anode was prepared by pressing the NiO-BCZSm powder and sintering at 1000 °C for 2 h.

Electrolyte membrane was prepared by spin coating with the KW-4A spin coating machine. The electrolyte slurry was distributed on the surface of the anode support under centrifugal force and annealed at 1450 °C for 5 h. A single cell was fabricated by co-sintering at 1000 °C for 2 h with a cathode layer coated on the sintered anode-supported BCZSm film.

Transmission Electron Microscopy (TEM) was used to show the size of BCZSm grains. Thermal Gravimetry Analysis-Differential Scanning Calorimetry (TGA-DSC) was used to determine the formation temperature of BCZSm phase. The structures of $La_{0.6}Sr_{0.4}Fe_{0.9}Nb_{0.1}O_3$ (1000 °C, 1150 °C), $BaCe_{0.7}Zr_{0.2}Sm_{0.1}O_{3-\alpha}$ (1400 °C) and NiO-BCZSm were analyzed via X–ray Diffraction (XRD).

The morphologies of $La_{0.6}Sr_{0.4}Fe_{0.9}Nb_{0.1}O_3$ (1150 °C) and the cross section of the thin-film fuel cell (LSFNb / BCZSm / NiO-BCZSm) were tested using a Scanning Electron Microscope (SEM). The H_2/O_2 fuel cell was tested at 700 °C and 800 °C.

3. RESULTS AND DISCUSSION

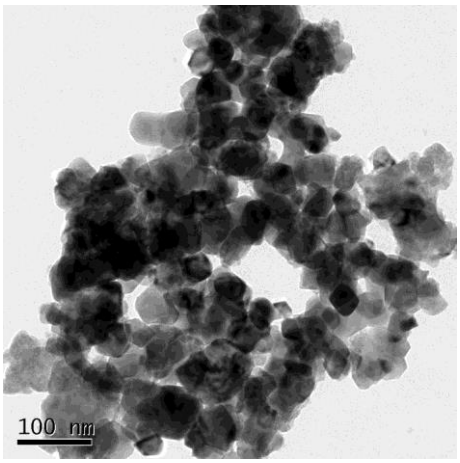

Figure 1. TEM graph of the BCZSm via a sol-gel method.

Fig.1 is the TEM graph to show the size of BCZSm grains. The TEM results show that many electrolyte particles were uniformly distributed. The reason is that the BCZSm electrolyte powder prepared by sol-gel method had a small particle size. Fig.1 indicates that the particle size of the BCZSm was 15-25 nm [7–8].

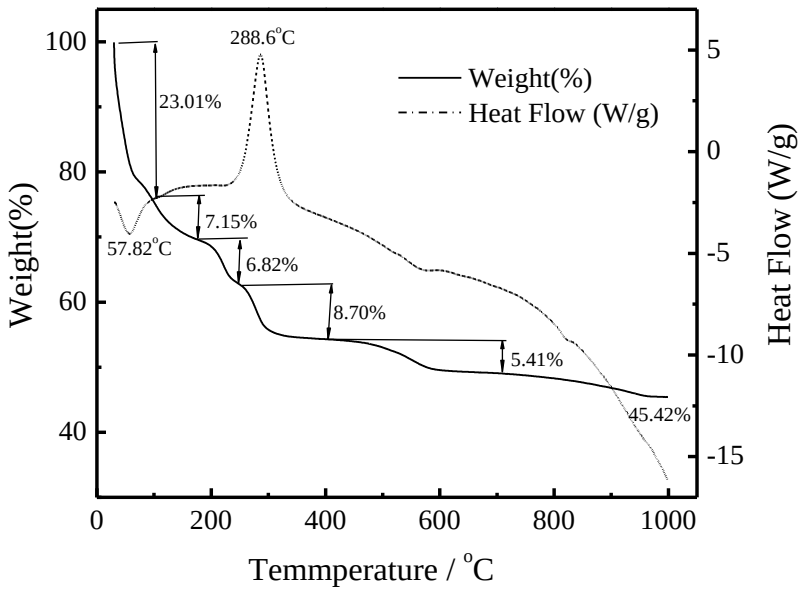

Figure 2. TGA-DSC curve of the BCZSm precursor from room temperature to 1000 °C.

Fig. 2 shows thermal decomposition of the BCZSm precursor during heating. The weight loss near 100°C was due to the heated dehydration and volatilization of the physically adsorbed water or other substances. The sharp exothermic peak at 288.6°C was caused by the decomposition of nitrates and organic compounds. The weak exothermic peak at 600-800°C was due to the process of continuous decomposition of nitrate. The weight hardly changed from 970°C, which indicates the formation of BCZSm crystal phase. Therefore, the first sintering temperature was 1100°C [22].

X-ray Diffraction patterns of $La_{0.6}Sr_{0.4}Fe_{0.9}Nb_{0.1}O_3$ (1000 °C, 1150 °C), $BaCe_{0.7}Zr_{0.2}Sm_{0.1}O_{3-\alpha}$ (1400 °C) and NiO-BCZSm are shown in Fig. 3. It can be seen that the $La_{0.6}Sr_{0.4}Fe_{0.9}Nb_{0.1}O_3$ cathode sample calcined at 1000 °C for 5 h formed a single-phase structure [14–15]. The spectrum of $BaCe_{0.7}Zr_{0.2}Sm_{0.1}O_{3-\alpha}$ (1400 °C) powder had a perovskite structure similar to that of $BaCeO_3$. This indicates that Zr and Sm can well replace Ce in the lattice structure. It can be seen that a composite structure of $BaCe_{0.7}Zr_{0.2}Sm_{0.1}O_{3-\alpha}$ and NiO formed in the sample of NiO-BCZSm anode.

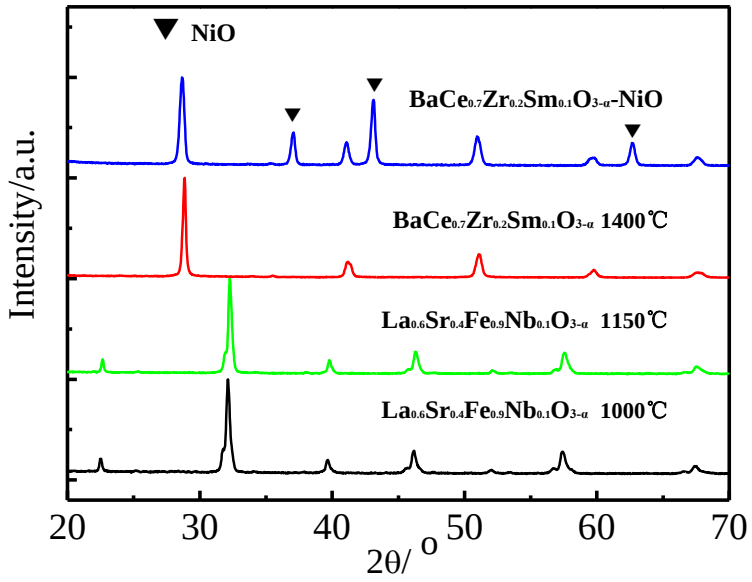

Figure 3. XRD patterns of $La_{0.6}Sr_{0.4}Fe_{0.9}Nb_{0.1}O_3$ (1000 °C, 1150 °C), $BaCe_{0.7}Zr_{0.2}Sm_{0.1}O_{3-\alpha}$ (1400 °C) and NiO-BCZSm.

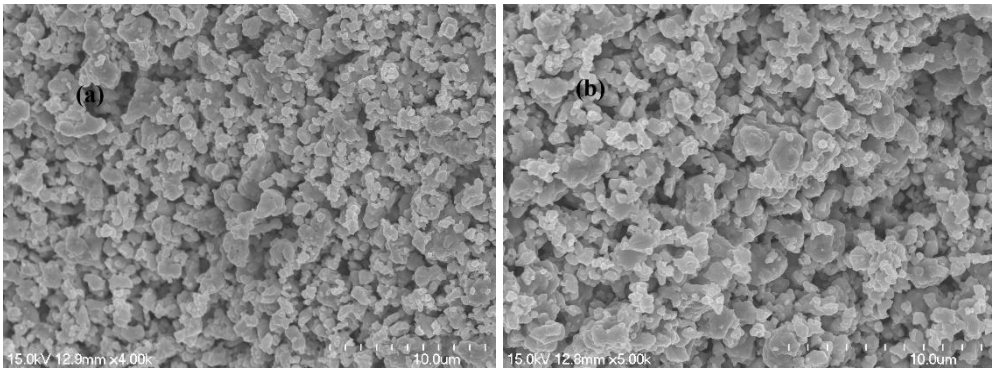

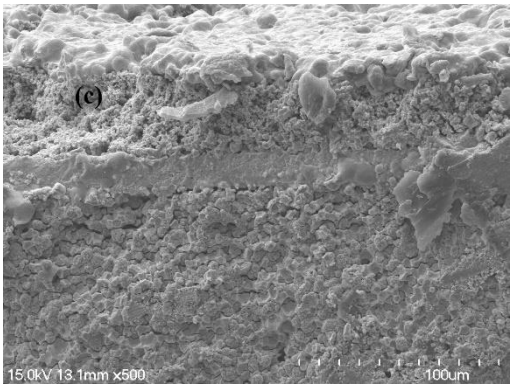

Figure 4. The surface and cross-sectional SEM photos of $La_{0.6}Sr_{0.4}Fe_{0.9}Nb_{0.1}O_3$ (1150 °C) and cross section of thin film fuel cell.

The surface and cross-sectional SEM photos of $La_{0.6}Sr_{0.4}Fe_{0.9}Nb_{0.1}O_3$ (1150 °C) and cross section of the thin-film fuel cell are shown in Fig. 4. The LSFNb cathode exhibited a homogeneous and appropriately porous microstructure. Fig. 4(c) is a SEM photograph of the cross section of the thin-film fuel cell (LSFNb / BCZSm / NiO-BCZSm) made of the LSFNb cathode, BCZSm electrolyte and NiO-BCZSm anode sintered at 1000 °C for 2 h [11–12]. It can be seen that the interface between the cathode material and electrolyte was well bonded. The BCZSm film was continuous and compact with a thickness of 18μm.

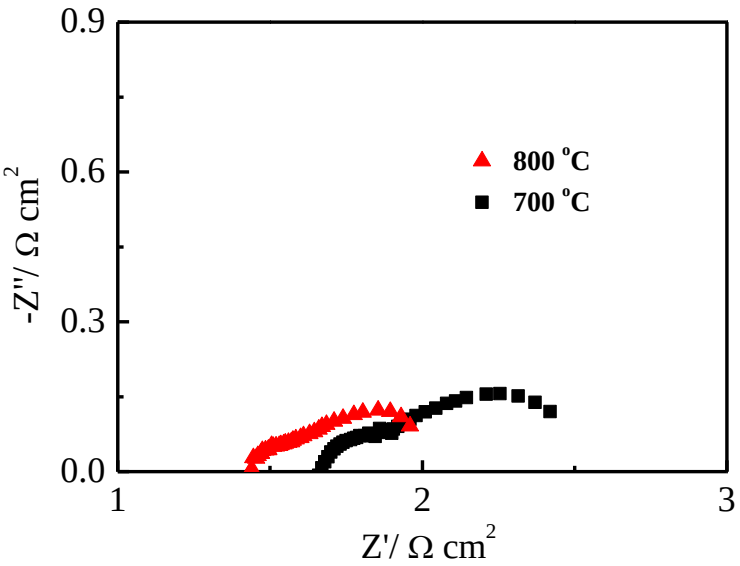

Figure 5. AC impedance diagrams of thin film fuel cell (LSFNb / BCZSm / NiO-BCZSm) under open-circuit conditions at 700 °C and 800 °C.

Fig. 5 shows the impedance spectra of the thin-film fuel cell (LSFNb / BCZSm / NiO-BCZSm) under open-circuit conditions at 700 °C and 800 °C. With the increase of temperature, the ohmic and polarization resistance decreased gradually. Total ohmic resistance is the high-frequency intercept of

impedance spectrum. The different values between high and low frequencies of the semicircle are the polarization resistance (R_p). The R_p of the thin-film fuel cell (LSFNb / BCZSm / NiO-BCZSm) under open-circuit conditions at 700 °C and 800 °C were 0.22 Ω·cm^2 and 0.16 Ω·cm^2, respectively.

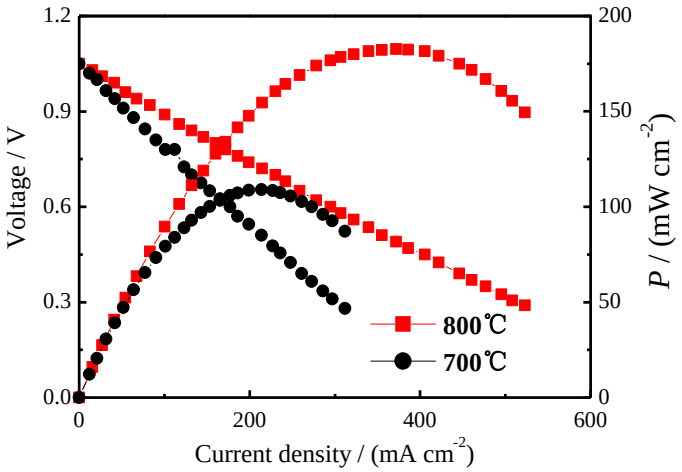

Figure 6. *I-V-P* curves of the H_2/O_2 fuel cells for thin film fuel cell (LSFNb / BCZSm / NiO-BCZSm) at 700 °C and 800 °C.

Table 1. The highest power densities of LSFNb / BCZSm / NiO-BCZSm and similar cathodes in the literatures.

cathodes	Highest power densities
$La_{0.6}Sr_{0.4}Fe_{0.9}Nb_{0.1}O_3$ (LSFNb)	182.6 mW·cm^{-2}, 800 °C, H_2 as fuel in this work
$(La_{0.6}Sr_{0.4})_{0.9}Co_{0.2}Fe_{0.6}Nb_{0.2}O_{3-\alpha}$	126 mW·cm^{-2}, 800 °C, CH_4 as fuel [17]
$La_{0.4}Sr_{0.6}Co_{0.2}Fe_{0.7}Nb_{0.1}O_{3-\alpha}$	54 mW·cm^{-2}, 850 °C, H_2 as fuel [20]
$La_{0.9}Ca_{0.1}Fe_{0.9}Nb_{0.1}O_{3-\alpha}$	322 mW·cm^{-2}, 800 °C, H_2 as fuel [19]

Fig. 6 shows the *I-V-P* curves of the H_2/O_2 fuel cells for the thin-film fuel cell (LSFNb / BCZSm / NiO-BCZSm) at 700 °C and 800 °C. The cell using BCZSm as the electrolyte reached the highest power densities of 109 mW·cm^{-2} and 182.6 mW·cm^{-2} at 700 °C and 800 °C, respectively. Meng et al. assembled a Ni-YSZ/YSZ/$La_{0.8}Sr_{0.2}MnO_{3-\delta}$-YSZ fuel cell and obtained approximately 100 mW·cm^{-2} at 700 °C [27]. The power output of ours was higher than those of $(La_{0.6}Sr_{0.4})_{0.9}Co_{0.2}Fe_{0.6}Nb_{0.2}O_{3-\alpha}$ (800 °C) using CH_4 as fuel [17] and $La_{0.4}Sr_{0.6}Co_{0.2}Fe_{0.7}Nb_{0.1}O_{3-\alpha}$ (850 °C) [20], however, it was lower than $La_{0.9}Ca_{0.1}Fe_{0.9}Nb_{0.1}O_{3-\alpha}$ (800 °C) [19] under the same condition (Table 1). This can be ascribed to the different cathode types. It shows that LSFNb has good catalytic activity and is suitable for medium temperature fuel cells.

4. CONCLUSIONS

In this study, a thin-film fuel cell of LSFNb / BCZSm / NiO-BCZSm was assembled using a novel cobalt-free $La_{0.6}Sr_{0.4}Fe_{0.9}Nb_{0.1}O_3$ (LSFNb) cathode material. The XRD analysis indicated that LSFNb and BCZSm formed a single-phase structure. The SEM photos of LSFNb cathode exhibited a homogeneous and appropriately porous microstructure. The BCZSm film was continuous and compact with a thickness of 18μm. The polarization resistances of the thin-film fuel cell under open-circuit conditions at 700 °C and 800 °C were 0.22 $\Omega \cdot cm^2$ and 0.16 $\Omega \cdot cm^2$, respectively.

References

1. G. L. Liu, W. Liu, Q. Kou and S. J. Xiao, *Int. J. Electrochem. Sci*., 13 (2018) 2641.
2. W. Zhang, M. Yuan, H. Wang and J. Liu, *J. Alloy Compd.*, 677(2016) 38.
3. Y. Tian, Z. Lü, X. Guo and P. Wu, *Int. J. Electrochem. Sci*., 14 (2019) 1093.
4. L. Sun, H. Wang, L. Sheng and H. Li, *Int. J. Electrochem. Sci.*, 12 (2017) 9689.
5. R. Shi, J. Liu, H. Wang, F. Wu and H. Miao, *Ceram. Int.*, 43 (2017) 16931.
6. T. Hibino, K. Kobayashi, P. Lv, M. Nagao and S. Teranishi, *Bull. Chem. Soc. Jpn.*, 90 (2017) 1017.
7. Q. Guan, H. Wang, H. Miao, L. Sheng and H. Li, *Ceram. Int.*, 43 (2017) 9317.
8. Y. N. Chen, T. Tian, Z. H. Wan, F. Wu, J. T. Tan and M. Pan, *Int. J. Electrochem. Sci.*, 13 (2018) 3827.
9. A.A. Solovyev, S.V. Rabotkin, A.V. Shipilova and I.V. Ionov, *Int. J. Electrochem. Sci*., 14 (2019) 575.
10. J. Li, H. Zhang, M. Gao, Q. Li, W. Bian, T. Tao and H. Zhang, *Materials*, 11 (2018) 749.
11. H. Ding and X. Xue, *J. Power Sources*, 195(2010) 4139.
12. H. Ding and X. Xue, *Int. J. Hydrogen Energ*., 35(2010) 2486.
13. H. Ding and X. Xue, *Int. J. Hydrogen Energ*., 35(2010) 4311.
14. C. Zhu, X. Liu, C. Yi, L. Pei, D. Yan, J. Niu, D. Wang and W. Su, *Electrochem. Commun.*, 11 (2009) 958.
15. K. Yao, X. Liu, P. Li, H. Liu, L. Gao, H. Wang, M. Zheng and W. Su, *Int. J. Hydrogen Energ*., 36(2011) 6123.
16. F. Zhang, Z.Yang, H.Wang, W.Wang and G.Ma, *Fuel Cells*, 12 (2012) 749.
17. B. Niu, F. Jin, T. Feng, L. Zhang, Y. Zhang and T. He, *Electrochim. Acta*, 270 (2018) 174.
18. Z. Yang, N. Xu, M. Han and F. Chen, *Int. J. Hydrogen Energ.*, 39(2014) 7402.
19. X. Kong, X. Zhou, Y. Tian, X. Wu, J. Zhang and W. Zuo, *J. Power Sources*, 326(2016) 35.
20. N. Xu, T. Zhu, Z. Yang and M. Han, *J. Mater. Sci. Technol.*, 33 (2017) 1329.
21. M. A. Haque, A. B. Sulong, E. H. Majlan, K. S. Loh, T. Husaini and R. Rosli, *Int. J. Electrochem. Sci*., 14 (2019) 371.
22. J. Xiao, L. Chen, H. Yuan, L. Ji, C. Xiong, J. Ma and X. Zhu, *Mater. Lett.*, 189 (2017) 192.
23. J. Lyagaeva, G. Vdovin, L. Hakimova, D. Medvedev, A. Demin and P. Tsiakaras, *Electrochim. Acta*, 251 (2017) 554.
24. I. Diaz-Aburto, F. Gracia and M. Colet-Lagrille, *Fuel Cells*, 19 (2019) 147.
25. F. Altaf, R. Batool, R. Gill, G. Abbas, R. Raza, Z. Rehman and M.A. Ahmad, *Ceram. Int.*, 45 (2019) 10330.
26. M. Anwar, Muhammed Ali S.A., A. Muchtar and M.R. Somalu, *Ceram. Int.*, 45 (2019) 5627.
27. X. Meng, X. Gong, N. Yang, X. Tan, Y. Yin and Z. Ma, *J. Power Sources*, 237 (2013) 277.